PERGAMON

Vacuum 57 (2000) 71–80

VACUUM
SURFACE ENGINEERING, SURFACE INSTRUMENTATION & VACUUM TECHNOLOGY

www.elsevier.nl/locate/vacuum

LEED study of Ni (1 0 0) and (1 1 1) surface damage caused by Ar^+ ion bombardment with low energy and small doses

M.A. Vasylyev*, A.G. Blaschuk, N.S. Mashovets, N.Yu. Vilkova

Institute of Metal Physics NAS of Ukraine, 36, Vernadsky Str., Kiev 252680, Ukraine

Abstract

Surface damage formation on the Ni (1 0 0) and Ni (1 1 1) surfaces induced by Ar^+ ion bombardment at low energy (0.1–1.2 keV) and small doses ($< 5 \times 10^{15}$ ion/cm^2) was studied with LEED. The degradation of the diffraction spot intensities was measured directly during ion bombardment. Using the procedure of Jacobson and Wehner for description of the exponential intensity/dose function, the mean area of damage per incident ion was determined. The experimental results have confirmed that partial annealing of the surface damage takes place at room temperature during ion bombardment. An exponential relationship observed between point defect concentration and annealing time at higher temperature indicated a first-order reaction. The activation energies for Ni (1 0 0) and Ni (1 1 1) surfaces were determined.

Keywords: Surface defects; Ion bombardment; Nickel surface; LEED; Defect annealing

1. Introduction

It is well known that the low-energy inert gas ion bombardment of solid surfaces is extensively used in several fields of surface science and technology. In particular, Ar^+, He^+, Ne^+ ion beams in the energy range $\sim$0.5–10 keV are frequently used in many surface techniques for producing atomic clean single-crystal faces [1–3] and to remove material quantitatively for obtaining layer-by-layer depth properties profiles [4,5]. Low-energy ion beams (probes or microprobes) are also applied in several surface analysis techniques, in particular, low-energy ion scattering (LEIS) and secondary ion mass-spectroscopy (SIMS) [6–9], or for ion-lithography technology [10]. The

* Corresponding author. Fax: + 38-044-444-2561.
E-mail address: vasil@imp.kiev.ua (M.A. Vasylyev).

0042-207X/00/$ - see front matter
PII: S0042-207X(00)00109-3

inert gas ion bombardment is used to change the chemical reactivity of the metal surfaces [11–13]. In the last few years low-energy ion treatment has found wide application in vacuum coating deposition technology [14–16].

Consequently, in order to understand the mechanisms of the ion-bombardment effects on a great diversity of surface structures and properties it is very important to study the nature of the surface damage produced by such treatment. It was established that in the case of semiconductors, ion bombardment can reduce the surface to a completely amorphous state [17,18]. In contrast to semiconductors it was demonstrated that the metal surface layers are never made amorphous although they can become partially disordered with increasing inert gas ion-bombardment dose [19–24]. However, there is not much quantitative data on metal surfaces because there are major difficulties arising from the high defect annealing rates even at room temperature in contrast to semiconductors. Moreover, there are difficulties in determining the type and concentration of the surface defects. The damage introduced by keV ion bombardment of a metal surface is expected to consist of vacancies, vacancy clusters, vacancy–ion complexes, interstitial agglomerates, Frenkel pairs, facets and dislocation loops [2,12,25]. The relation between various types of defects is dependent on the type of metal and ion as well as ion energy and dose of the bombardment.

To study low-energy ion damage processes which involve only a few surface layers an important technique is low-energy electron diffraction (LEED). LEED has been shown to be capable of providing information about the height of atomic steps, and to some extent about the width of terraces on atomically clean surfaces [26]. Previous LEED studies of the surface damage caused by ion bombardment have demonstrated that such treatment can change both the intensity and the width of the diffracted beam (spots) [19,20]. Jacobson and Wehner [17] first examined the effect of Ar^+ ion bombardment of the Ge (1 1 1) surface at energies up to 1 keV. The intensity distribution of LEED beams in the energy range 15–200 eV was the particular measurement in this study. It was found that an exponential decrease of the diffraction spot intensity with increasing ion dose was seen. They also observed that, if the energy of bombarding ions was increased, the ion dose required to produce a given reduction in intensity, decreased. These results were explained using a model in which it was speculated that each incoming ion creates a certain damaged area of size a. According to this model, the fraction of the surface which is damaged, θ, is given by

$$\mathrm{d}\theta/\mathrm{d}D = (1 - \theta)a, \tag{1}$$

where D is the ion-bombardment dose. Solving this equation one can obtain

$$\theta = 1 - \exp(-a\,D), \tag{2}$$

i.e., the non-damaged area, $1 - \theta$, decays exponentially with ion dose in terms of this model.

Park [19] has studied the effect of Ar^+ ions with 500 eV bombardment on the LEED intensity for a clean annealed (1 0 0) Ni surface. He found that, even at extremely high ion dose, the LEED pattern was never completely destroyed. It was suggested that the ion bombardment produces a random distribution of point defects in an initially perfect plane surface. This reduces the effective scattering area of the surface and will result in a decrease in diffraction intensities. However, the undamaged portions of the surface area are in registry with one another and scatter cooperatively. Therefore, the diffraction beam width due to bombardment will not be appreciably affected in this

case. The beam broadening observed by Park [19] was explained by assuming a lattice strain caused by Ar atoms embedded in the lattice.

In studies [20,21] Ne^+, Ar^+, Kr^+ or Xe^+ ion-bombardment induced-damage on Mo (0 1 1), (1 1 0) and W(1 1 0) surfaces was investigated also by LEED. Degradation, determined from peak intensities, was observed as a function of ion dose and energy in the range 25–1000 eV. Using the procedure of Jacobson and Wehner [17], the mean area of damage per incident ion was observed to be $\sim 0.6 \times 10^{-15}$ cm^2/ion at 50 eV for both Ne^+ and Xe^+, and at 1000 eV 25×10^{-15} cm^2/ion for Ne^+ and 9×10^{-15} cm^2/ion for Xe^+. LEED patterns from both surfaces of bombarded Mo were restored by heating at 873–923 K. It was also found that beam broadening occurred mainly with neon and, was a function of ion dose. The present results also agree with those of Park [19] and, even at extremely high ion doses, the LEED pattern was never completely destroyed because the undamaged areas that exist still scatter cooperatively.

The production and annealing of damage on the Ni (1 1 0) surface, induced by 1 keV Ar^+ bombardment has been studied with LEED [23,24] and the results were discussed and compared with previously reported LEIS results [24]. It was concluded that the production of damage on crystal surfaces which remain crystalline under ion bombardment may be explained in terms of the nucleation and growth of vacancy clusters. After bombardment at a dose of about 10^{15} ion/cm^2, extra LEED pattern spots were observed which were interpreted as being due to the formation of steps and facets.

In the work of Verheij et al. [24] the thermal annealing of Ni (1 1 0) surface damage was also studied using LEIS. The separate role of thermal processes was investigated by measuring changes in the height of the damage LEIS peaks following cessation of bombardment for different target temperatures. For complete annealing of the nickel surface damage, the target had to be heated to 450 K. The data presented [23,24] were, however, not very sensitive to annealing effects because of the time delay between bombardment and measurement ($\sim$10 min) and because peak intensities during annealing could not be measured accurately, since the adverse effects of the Debye–Waller factor and lattice thermal expansion were not considered. Moreover, the effect of annealing (in the interval between bombardment and measurement) on the damage built-up during ion bombardment even at room temperature cannot be neglected in quantitative experiments. The aim of the present work was to perform more precise measurements of the LEED intensities directly during the ion-bombardment process and subsequent damage annealing. Because of the low-energy ions and low doses used it is expected that only point defects were produced.

2. Experimental

The targets used were high-purity (5N) Ni (1 0 0) and (1 1 1) surfaces, prepared by standard techniques. The crystals with dimensions $10 \times 10 \times 3$ mm were mechanically polished using 6 μm diamond paste and finally given prolonged electropolishing. This treatment produced smooth specular surfaces. The samples were then spot welded on to tungsten supports and inverted into the LEED-AES spectrometer [27]. The target surface preparation in the UHV chamber involved several sputtering cycles with Ar^+ (600 eV) and annealing (900 K), and a final treatment with oxygen at an O_2 pressure $P = 1 \times 10^{-6}$ Pa for 15 min with the sample at 750 K. The surface was considered clean when no traces of oxygen were detectable, the ratio of the Auger carbon peak to

that of the nickel 848 eV peak was kept below 5×10^{-3}, and a clear (1×1) LEED pattern observed did not change after further cleaning treatment.

In order to enhance the performance of the LEED system, in particular, the sensitivity and accuracy, compared to conventional LEED apparatus, we have performed several improvements in the diffraction reflex (spot) intensity measurements. Let us briefly focus here our attention on such improvements. In order to study the LEED reflex behaviour under ion bombardment and subsequent heating, both the reflex intensity and shape must be measured. With this aim in view we have developed a special spot-photometry device. Numerous experiments on the temperature dependence of the spot intensity have shown that the temperature range of investigation is limited by light from the heated sample. In order to exclude this error we have developed the technique of intensity modulation of LEED spots. Furthermore, when investigating the temperature or ion dose dependences of the diffraction spot intensity, the expansion of the crystal lattice must be taken into account since this causes shifting of the energy maxima of the spots. Because of this, a system of automatic energy adjustment to the spot maximum intensity during experiments was developed. These improvements allow one to record the spot intensity maximum variation with ion-bombardment dose, target temperature, and annealing time. The target heating facility, comprising a simple electron gun mounted behind the target, allowed the temperature to be maintained constant in the range between 300 and 1000 K to an accuracy of ± 2 K.

To damage the target surface, it was bombarded with Ar^+ ions at an angle of incidence of 45°. The argon gas pressure in the UHV chamber was $(2\text{–}4) \times 10^{-3}$ Pa during the bombardment. The ion energy E_p and dose D were varied from 0.1 to 1.2 keV and from 10^{13} to 10^{16} ion/cm^2, respectively.

3. Results and discussion

An important point is that we have performed for the first time the LEED measurement directly during ion bombardment. The LEED patterns, were observed slightly off normal electron beam incidence (7°) to allow study of the (0 0) specular reflection with the primary electron energy E_0 between 10 and 200 eV. At the first stage of the study we have performed detailed measurement of the ion dose dependence of both the (0 0) spot intensity and its width. It was shown that, for this energy range (E_0), the spatial spot profile did not vary over low ion doses $D < 5 \times 10^{15}$ ion/cm^2. However, a slight variation in spot size, i.e. beam broadening, was detected on the $I_{00}(E_0)$-curves particularly at higher doses. For higher dose level also the peak energy shifts towards higher energies by 2–5 eV. So, for $D < 5 \times 10^{15}$ ions/cm^2, the ion bombardment mainly affected the spot intensities which were then measured in more detail. Fig. 1 shows some typical examples of the intensity dependence on bombardment time, i.e. the dose-dependent relationship for $E_p = 0.5$ keV, $E_0 = 96$ eV. One can see that the main effect caused by ion bombardment is the decrease of the spot intensity during the bombardment process. It was found for several $I(t)$ functions that for each E_p, there is an inherent maximum dose value above which the intensity does not alter, i.e. a saturation condition is reached. This final intensity value was usually 0.2 of the initial intensity I_0. We have followed the same procedure as performed by Jacobson and Wehner [17], where the $I(D)$ function was described by the exponential behaviour expected from Eq. (1). It was assumed that surface damage is caused by build-up of the point defects. We have plotted I/I_0 vs. dose on

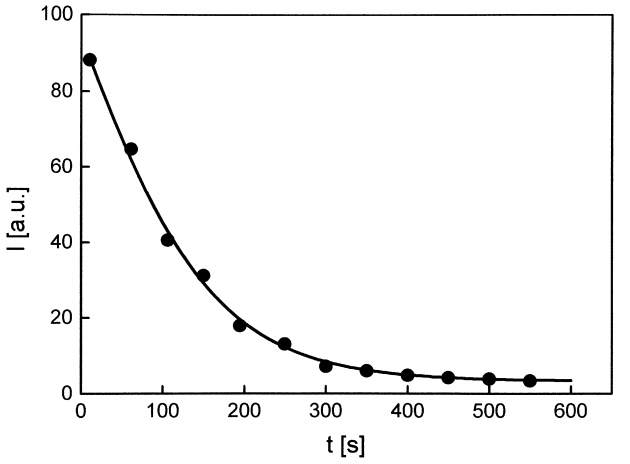

Fig. 1. LEED (0 0) spot intensity as a function of Ar^+ ion-bombardment time. $E_p = 0.5$ keV.

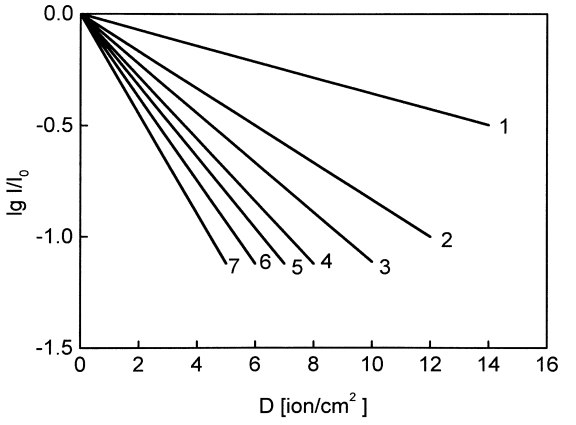

Fig. 2. $-\log(I/I_0)$ as a function of bombardment dose for Ni (1 0 0). E_p in keV. (1) 0.1, (2) 0.2, (3) 0.3, (4) 0.4, (5) 0.5, (6) 0.6, (7) 1.2. $E_0 = 96$ eV.

a semi-log scale which indicated that I/I_0 values were a straight line, at least in the region of small doses. Fig. 2 shows a number of the representative straight lines $\ln(I/I_0) = f(D)$ for the Ni (1 0 0) surface at several ion energy values. As mentioned above, the mean area damaged per incident ion ($\tilde{a}$) may be obtained from the slope of the $-\log(I/I_0)$ vs. dose in ions/cm^2. As shown in Fig. 3 for Ni (1 0 0) and Ni (1 1 1) surfaces $\tilde{a}$ increases monotonically in the range of E_p from 0.1 to 1.0 keV. One can see from Fig. 3 that the defect formation effect for the closer-packed (1 1 1) face is less than that for the (1 0 0) face. The $\tilde{a}$ value measured 10 min after ion bombardment at room temperature was less by an order of magnitude than that in Fig. 3. These results give a clear indication that fast thermally activated process are occurring even at room temperature.

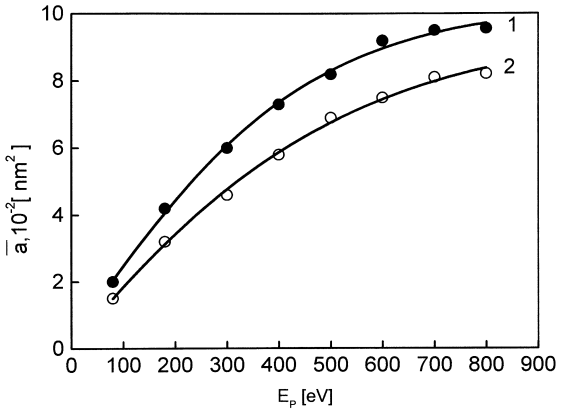

Fig. 3. Mean damage area per ion a as a function of E_p for (1) Ni (1 0 0) and (2) Ni (1 1 1).

The separate role of the thermal process kinetics was investigated by measuring changes in the (0 0) spot intensity at $E_0 = 96$ eV for Ni (1 0 0) or $E_0 = 87$ eV for Ni (1 1 1) during isothermal annealing following cessation of bombardment at room temperature. The defects were produced before annealing by bombardment with 600 eV Ar^+ at a dose of 8×10^{14} ions/cm^2. Once a given dose has been reached equal to the saturation damage level, the ion beam was switched off and the specimen was heated to the annealing temperature. The (0 0) spot intensity $I(t)$ was recorded from the start of annealing until a stable value of $I_{st}(t)$ was attained. The sets of the isothermal curves for different annealing temperatures for both crystals are displayed in Fig. 4a,b. A distinct increase in spot intensity, indicating accurately surface damaged annealing, was observed over the entire temperature range used, i.e. from 400 up to 900 K. It is also seen in Fig. 4 that the $I(t)$-function allows the annealing curves to be characterized by a time constant, above which no damage was observed. Measurements at several temperatures have shown that this time constant decreased with increasing annealing temperature. All curves for different T reach finally saturation values as seen in Fig. 4. On the other hand, the times required for saturation depend strongly on annealing temperature. In order to determine the defect-annealing parameters we used the relation between the LEED intensity and the point defect concentration n [17]:

$$I_T(t) = I_{0T}\,[1 - \tilde{a}n(t)^2]. \tag{3}$$

A plot of $\ln[1 - (I_T/I_{0T})^{1/2}]$ as a function of time t for fixed $\tilde{a}$ enables one to determine a direct relationship between n and t. Fig. 5 shows such a function for Ni (1 1 0) as derived from the data in Fig. 4. One can see in Fig. 5 that all isotherms are drawn as straight lines. Analogous results were obtained for Ni (111). Hence, the data points for n fit rather well to an exponential function, i.e.

$$n = n_0 \exp(-t/\tau), \tag{4}$$

where τ is the temperature which is dependent on the mean lifetime of the defect. As already known [28] the defect-annealing behaviour for a single activation energy ε is described by the equation

$$\mathrm{d}n/\mathrm{d}t = K_0 n^{\alpha} \exp(-\varepsilon/kT), \tag{5}$$

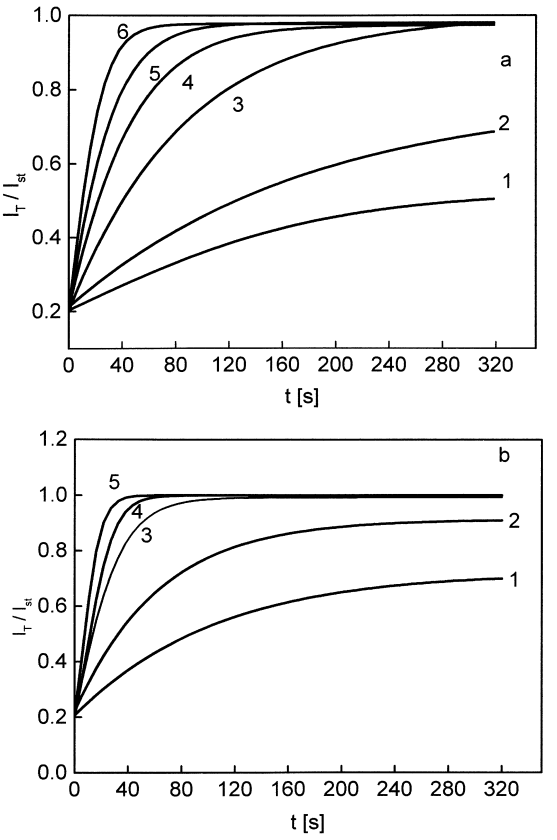

Fig. 4. Intensity ratio (I/I_0) as a function of isothermal annealing time: (a) Ni (1 0 0), (b) Ni (1 1 1) at temperatures in K (1) 400, (2) 500, (3) 600, (4) 700, (5) 800, (6) 900.

where K_0 is the kinetic coefficient, k the Boltzmann constant, and α the reaction order; if the defects diffuse to a fixed number of sinks, $\alpha = 1$. Vacancy and interstitial-atom annihilation corresponds to the second order ($\alpha = 2$) if these defects have equal concentrations. It is very important to know the numerical values of the reaction order in order to analyze the defect-annealing behaviour. Integrating Eq. (5) gives

$$n = n_0 \exp(-t/\tau),$$

$$\tau = K_0^{-1} \exp(\varepsilon/kT) \quad \text{for } \alpha = 1$$

and

$$1/n^{\alpha-1} - 1/n_0^{\alpha-1} = (\alpha - 1)\, K_0 (t - t_0) \exp(-\varepsilon/kT)$$

for $\alpha \neq 1$.

Consequently, the above-mentioned exponential relationship between n and t, indicates a first-order reaction in our case. The section applied to the isotherms gives $\ln \tau$ as a function of $1/T$,

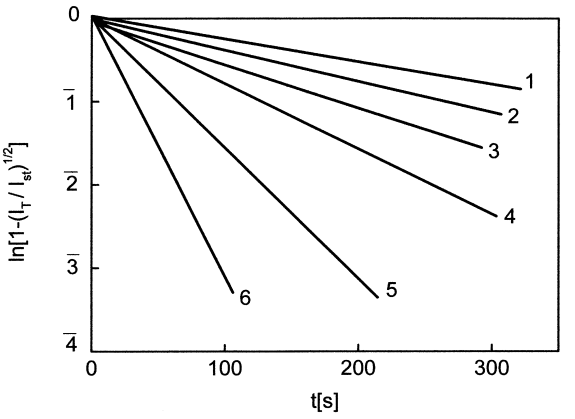

Fig. 5. $-\ln[1-(I/I_0)^{1/2}]$ as a function of annealing time for fixed $\tilde{a}$ for Ni (1 1 1) at temperatures in K (1) 400, (2) 500, (3) 600, (4) 700, (5) 800, (6) 900.

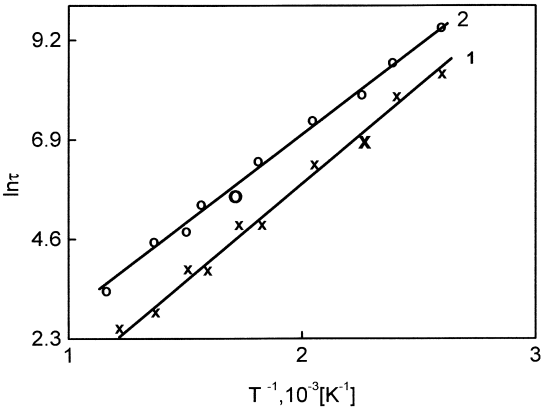

Fig. 6. $\ln\tau$ as a function of $1/T$: (1) Ni (1 0 0), (2) Ni (1 1 1).

which is a straight line with a slope equal to ε/k (Fig. 6). From these data the values of ε for Ni (1 0 0) and Ni (1 1 1) were determined to be 0.3 and 0.25 eV, respectively.

It is well known that although LEED intensities are very sensitive to low-energy ion-bombardment damage, they do not distinguish between the various types of surface defects. However, we might expect, based on the low reaction order observed, that ion bombardment at both low E_p and D produces only simple point defects, mainly vacancies and close Frenkel pairs. Under thermal activation, the Frenkel pairs vanish without reacting with other types of defects, and ε may be of the order of the migration energy for interstitial atoms E_m^i (0.15 eV for nickel) because of the attraction between vacancies and interstitial atoms [28]. Point defects in the form of vacancies may be produced by low-energy ion bombardment at small doses, when only 1–2 surface monolayers are

sputtered. It is well known that vacancies control the diffusion process in the solid. In particular, the activation energy for self-diffusion, E_D, is given by [28]

$$E_D = E_f^V + E_m^V, \tag{6}$$

where E_f^V is the formation energy of a vacancy and E_m^V is the migration energy of a vacancy. On the other hand, the relation between the formation energy of a vacancy and the activation energy of self-diffusion is given by [29]

$$E_f^V = 0.55\, E_D. \tag{7}$$

The values of the activation energy of self-diffusion for Ni (1 0 0) and (1 1 1) surfaces, E_D^S, were determined in the study [30] to be equal to 0.63 and 0.33 eV, respectively. As the migration energy of a vacancy has not been documented for Ni we have used relations (6) and (7) to calculate this parameter. It was found that the values of E_m^V for Ni (1 0 0) and (1 1 1) faces are 0.15 and 0.29 eV, respectively. In the much studied case of Cu [28] the values of E_m^V were determined for (1 0 0) and (1 1 1) surfaces to be equal to 0.171 and 0.655 eV, respectively. These values are large in comparison with bulk data: 1.21 eV for Ni and 0.91 eV for Cu [29].

4. Conclusions

1. Surface damage on the Ni (1 0 0) and (1 1 1) surfaces induced by Ar^+ ion bombardment at low energy and small doses were studied with LEED. We report here the first observation of the (0 0) diffraction peak degradation directly during ion bombardment using the more precise measurements of the LEED intensities. The main effect caused by ion bombardment in the ion energy range 0.1–1.2 keV and for doses $< 5 \times 10^{15}$ ion/cm^2 is the exponential decrease of spot intensity, which did not approach zero for increasing dose. Under present conditions the equilibrium reached between the rate of the surface damage build-up and annealing. The results give a clear indication that fast thermally activated processes are occurring even at room temperature under ion bombardment. Using the procedure of Jacobson and Wehner for description of the exponential intensity/dose function, the mean area of damage per incident ion was determined.
2. Thermal process kinetics was investigated directly during isothermal annealing following the cessation of ion bombardment at room temperature. An exponential relationship between the number of point defects and annealing time indicated a first-order reaction. Activation energies for Ni (1 0 0) and Ni (1 1 1) were determined to be 0.3 and 0.25 eV, respectively. We might expect, based on the data observed, that ion bombardment at both low ion energy and small doses produces only simple point defects, mainly vacancies and close Frenkel pairs.

Acknowledgements

The work was performed as part of an INCOCOPERNICUS Network COATRANS, Contract ERBIC 15 CT98 0815.

References

[1] Farnsworth HE, Schlier RE, George T, Burger RJ. Appl Phys 1958;29:1150–61.
[2] Carter G, Colligon JS, Grant WA, Whitton JL. Radiat Res Rev 1971;3:1–68.
[3] Vasiliev MA. J Phys D 1997;30:3037–70.
[4] Lam N. Surf Interface Anal 1998;12:65–77.
[5] Hill M. Surf Interface Anal 1998;12:21–6.
[6] Carstanjen H. Nucl Instr and Meth B 1998;136–138:1183–90.
[7] O'Connor D, King B, MacDonald RJ, Shen Y, Chen X. Aust J Phys 1990;43:601–15.
[8] Webb A, Smith J. Surf Interface Anal 1998;12:303–8.
[9] Svensson B, Linnarsson M, Cardenas J, Petravic M. Nucl Instr and Meth B 1998;136–138:1034–9.
[10] Matsui S, Ochiai Y. Nanotechnology 1996;7:247–58.
[11] Cherepin VT, Kosyachkov AA, Vasiliev MA. Surf Sci 1976; 58:609–12.
[12] Miranda R, Rojo J. Vacuum 1984;34:1069–79.
[13] Chenakin SP. Vacuum 1986;36:635–41.
[14] Treglio J, Perry A, Stinner R. Adv Mater Proc 1995;5:29–32.
[15] Laimer J. Vacuum 1990;40:27–32.
[16] Wang X, Chen B. Vacuum 1994;45:23–8.
[17] Jacobson R, Wehner KG. J Appl Phys 1965;36:2674–5.
[18] Davidson SJ. Mater Sci 1972;7:473–4.
[19] Park RJ. Appl Phys 1966;37:295–8.
[20] Farnsworth H, Hayek K. Surf Sci 1967;8:35–56.
[21] Bellina J, Farnsworth HJ. Vacuum Sci Technol 1972;9:616–9.
[22] Heiland W, Taglauer E. Radiat Effects 1973;19:1–5.
[23] Verheij LK. Surf Sci 1982;114:667–72.
[24] Verheij LK, Van den Berg JA, Armour DG. Surf Sci 1982; 122:216–34.
[25] Karpuzov DS, Armour DG. J Phys D 1984;17:853–62.
[26] Henzler M. Appl Surf Sci 1982;11–12:450–69.
[27] Vasiliev MA, Gorodetsky SD. Vacuum 1987;37:723–8.
[28] Wynblatt P, Gjostein NA. Surf Sci 1968;12:109–27.
[29] Doyama M, Koehler JS. Acta Met 1976;24:871–9.
[30] Tung RT, Graham WR. Surf Sci 1980;97:73–9.